




Absolute frequency measurement of the $6s6p\ ^3P_0 \rightarrow 5d6s\ ^3D_1$ transition based on ultracold ytterbium atoms

Di Ai ¹, Taoyun Jin,¹ Tao Zhang,¹ Limeng Luo,¹ Luhua Liu,¹ Min Zhou ¹, and Xinye Xu ^{1,2,*}

¹State Key Laboratory of Precision Spectroscopy, East China Normal University, Shanghai 200241, China

²Shanghai Branch, Hefei National Laboratory, Shanghai 201315, China



(Received 31 January 2023; accepted 2 June 2023; published 12 June 2023)

The 1389-nm laser is used as a repumping laser in the ^{171}Yb optical lattice clock, which corresponds to the $6s6p\ ^3P_0 \rightarrow 5d6s\ ^3D_1$ transitions. To our knowledge, there is no report on the absolute frequencies for this repumping transition yet. We excite the hyperfine structure transitions with a 1389-nm scannable laser, which is stabilized on an absolute frequency-stabilized optical frequency comb, and obtain the transition spectra. The minimum spectral linewidth is around 705 kHz, which is approximately 1.5 times greater than the natural linewidth of 484 kHz. Based on evaluating the systematic frequency shifts precisely and referencing the frequency measurement results on the secondary representation of the International System of Units second, we are the first to report the direct measurement of the absolute frequencies for $6s6p\ ^3P_0$ ($F = 1/2$) \rightarrow $5d6s\ ^3D_1$ ($F = 1/2, 3/2$) transitions are $215\,875\,746.15 \pm (0.21)_{\text{stat}} \pm (0.06)_{\text{sys}}$ MHz and $215\,872\,697.14 \pm (0.11)_{\text{stat}} \pm (0.06)_{\text{sys}}$ MHz, respectively. In addition, the hyperfine splitting and magnetic dipole coefficient A of the $5d6s\ ^3D_1$ state is determined as $3049.01(26)$ MHz and $-2032.67(17)$ MHz, which is more accurate than the previous measurements by an order of magnitude.

DOI: [10.1103/PhysRevA.107.063107](https://doi.org/10.1103/PhysRevA.107.063107)

I. INTRODUCTION

Benefiting from the unprecedented measurement precision and accuracy [1–5], optical atomic clocks are of fundamental importance to fields as varied as time and frequency metrology [6–9], relativistic geodesy [10,11], and tests of fundamental physics [12–16]. The optical atomic clocks are realized by stabilizing a laser frequency to an atomic resonance based on measured transition probabilities [17]. In consideration of the long lifetime of the excited state for the selected clock transitions, it typically needs an additional laser to repump the atoms back to the ground state. For example, in the ^{171}Yb atomic clock, one could use a 1389-nm repumping laser to drive the population back to the ground state through the $^3P_0 \rightarrow ^3D_1 \rightarrow ^3P_1 \rightarrow ^1S_0$ channel [18,19]. Therefore, accurately determining the frequency of the repumping laser will be helpful to improve the repumping efficiency. Thereby, the excitation fraction of the obtained normalized clock transition spectra will reflect the true excitation rate of the clock interrogation and is not restricted by the repumping process.

^{171}Yb is a fermion with a nuclear spin of $I = 1/2$. The presence of additional structures to the states is shown in Fig. 1, and each $^{2S+1}L_J$ state will contain multiple levels denoted by quantum number F , where $F = |I \pm J|$. The frequency shift due to the hyperfine structure can be computed according to [20]

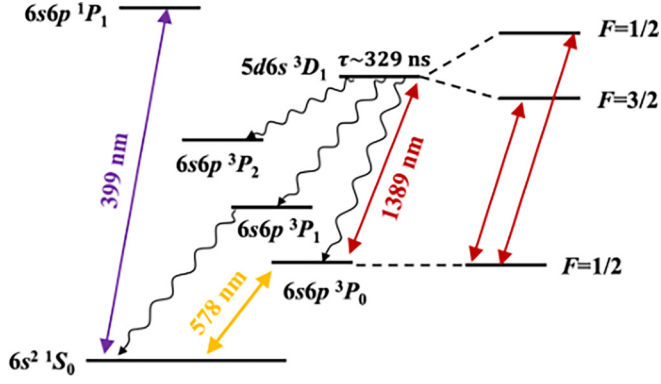
$$\Delta\nu = \Delta E_{\text{HFS}}/h = \frac{A}{2}K, \quad (1)$$

where A is the magnetic dipole coefficient and $K = F(F+1) - I(I+1) - J(J+1)$. The magnetic dipole coefficient A for the $5d6s\ ^3D_1$ state is shown in Table I, in which the values derived by theory and experiment disagree significantly. According to Eq. (1) and the theoretical value of A from Ref. [21], the frequency shifts of the $5d6s\ ^3D_1$ hyperfine structures are $\Delta\nu(^3D_1, F=1/2) = -A = 2349$ MHz and $\Delta\nu(^3D_1, F=3/2) = A/2 = -1174.5$ MHz, and the corresponding hyperfine splitting is 3524 GHz. However, some experimental measurements for the magnetic dipole coefficient A showed different results. By using the measured coefficient A , which is measured by hot atoms in Ref. [22], we will get a different hyperfine splitting around 3060(3) MHz. Moreover, a rough measurement of the hyperfine splitting from the cold ytterbium atoms is 3070(70) MHz [23].

Here we present a framework for directly measuring the absolute frequencies of the $6s6p\ ^3P_0$ ($F = 1/2$) \rightarrow $5d6s\ ^3D_1$ ($F = 1/2, 3/2$) transitions based on a ^{171}Yb lattice clock. Thereby, we determine the hyperfine splitting of the $5d6s\ ^3D_1$ state and extrapolate the corresponding magnetic dipole coefficient A . Our measurement results of A improve the accuracy by an order of magnitude compared to the previous results, but disagree with the most accurate measurement result from Ref. [22] by about four times combined uncertainty.

This work is structured as follows. Section II introduces the experimental setup and the detection of the transition spectra. Section III gives a detailed investigation of the systematic frequency shifts and corresponding uncertainties for the $6s6p\ ^3P_0$ ($F = 1/2$) \rightarrow $5d6s\ ^3D_1$ ($F = 1/2, 3/2$) transitions. In Sec. IV, the absolute frequencies are measured, followed by the determination of the hyperfine constant. We summarize with concluding remarks in Sec. V.

*xyxu@phy.ecnu.edu.cn

FIG. 1. The relevant energy levels of ^{171}Yb .

II. EXPERIMENTAL SETUP AND TRANSITION SPECTRA

The schematic of the experimental setup is shown in Fig. 2(a). The method for producing the cold atoms of ^{171}Yb has been described in our previous works [24,25]. A brief description is given here. We first cool the hot ytterbium beam with a Zeeman slower and three-dimensional magnetic optical trap (MOT) on the $^1S_0 - ^1P_1$ transition at 399 nm. The atoms are further cooled with a three-dimensional MOT operating on the $^1S_0 - ^3P_1$ transition at 556 nm. After that, the atoms are loaded into a one-dimensional optical lattice at the magic wavelength for the $^1S_0 - ^3P_0$ clock transition of ^{171}Yb .

The time series are shown in Fig. 2(b). We employ the electron-shelving technique [26] and use a 399-nm probe laser to detect the population of the atoms and collect the laser-induced fluorescence by a photomultiplier tube (PMT). After loading cold ytterbium atoms in a one-dimensional optical lattice, we employ a 578-nm pulse to excite atoms to the 3P_0 state. Subsequently, the first pulse of the 399-nm probe laser is applied to detect the remaining population of the 1S_0 state and record it as P_1 . We assume that the excitation fraction of the $^1S_0 - ^3P_0$ transition is η_1 , which remains constant during the measurements. Therefore, the population of atoms in 3P_0 at this time can be expressed as $P_1\eta_1/(1-\eta_1)$. Then, the $^3P_0 \rightarrow ^3D_1$ transition is driven by a 1389-nm laser. After that, the second 399-nm pulse is employed to detect the population P_2 , which implies that the atoms go back to the ground state through the $^3P_0 \rightarrow ^3D_1 \rightarrow ^3P_1 \rightarrow ^1S_0$ channel. The last 399-nm pulse is to detect the background atoms and record them as P_3 . Eventually, the excitation fraction of the $6s6p\ ^3P_0 \rightarrow 5d6s\ ^3D_1$ transition can be expressed as $\eta_2 = (P_2 - P_3)/[P_1\eta_1/(1-\eta_1) - P_3]$.

The frequency of the 1389-nm laser is stabilized on an optical frequency comb [27]. We selectively excited atoms to

TABLE I. The magnetic dipole (A) coefficient of ^{171}Yb for the $5d6s\ ^3D_1$ state.

	A (MHz)	Ref.
Theory	-2349	[21] (2019)
Experiment	-2040(2)	[22] (1999)
	-2047(47)	[23] (2012)
	-2032.67(17)	This work

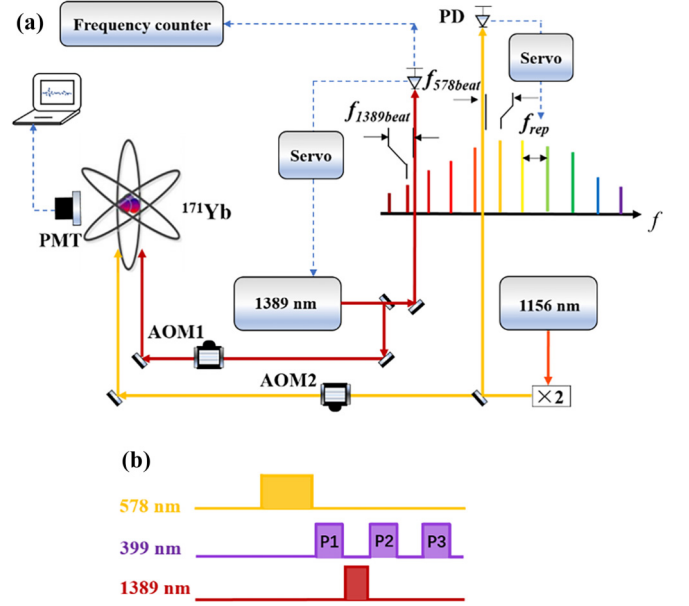


FIG. 2. Schematic of the experimental setup for frequency measurement. (a) The 1156-nm laser is prestabilized on a 30-cm ultra-low-expansion cavity [28]. After frequency doubling, the 578-nm laser is sent to a comb and the lattice trap separately. The frequency of AOM2 is fixed to ensure the 578-nm laser is constantly in resonance with the atoms during the measurement. Optical paths are depicted by solid lines; electric signals are shown by dashed lines. PD: photonic detector. (b) The relevant time series.

either of the hyperfine states 3D_1 ($F = 1/2, 3/2$) by tuning the 1389-nm laser and locking its frequency on the different teeth of the comb. Building on this foundation, the transition spectra are performed by scanning the rf driver frequency of the acoustic optical modulator [AOM1 shown in Fig. 2(a)] before the chamber within a small range. As the obtained spectral linewidth is wider than the natural linewidth of the transition at 484 kHz (natural linewidth $\gamma = 1/2\pi\tau$, the lifetime of the $5d6s\ ^3D_1$ state $\tau = 329$ ns [23]), we further investigate the broadening effect. Figures 3(a) and 3(b) show the linewidth of the spectra dependence on the intensity I and time duration T of the 1389-nm laser pulse. We could find that the width of the spectra is not dominated by the intensity broadening effect when set I at 0.08 nW/mm 2 . Furthermore, we observe that the linewidth will decrease with the reduction of T for both transitions. After optimizing the intensity and time duration of the 1389-nm beam, the obtained spectra for both transitions with the minimum measured linewidth are shown in Figs. 3(c) and 3(d). We fit the spectra with the Lorentzian function, and the minimum linewidth of the spectra is around 705 kHz, which is 1.5 times wider than the natural linewidth.

III. SYSTEMATIC SHIFTS

When we consider the absolute frequency for a specific atomic transition, the frequency shifts induced by various systematic effects cannot be ignored [29,30]. These shifts and uncertainties are evaluated by varying one experimental parameter at a time and scanning the resonance transition ten times continuously. Then the average center frequency f_c of

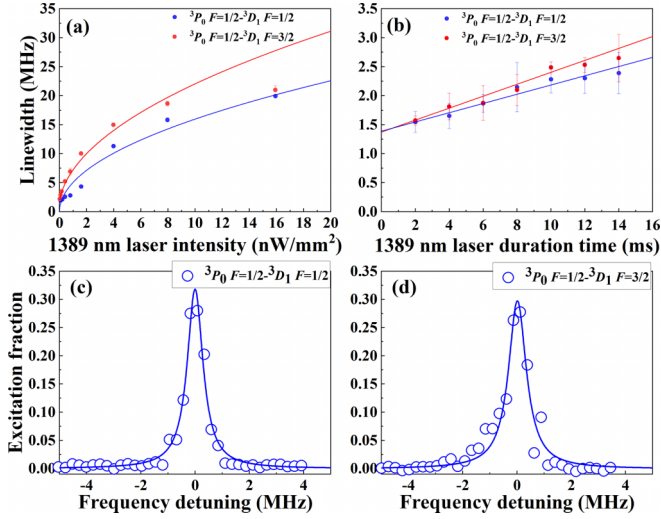


FIG. 3. The spectra and measured linewidth of the $6s6p\ ^3P_0 \rightarrow 5d6s\ ^3D_1$ transitions as a function of the 1389-nm beam intensity I and time duration T . (a) Linewidth dependent on intensity I with $T = 12$ ms. (b) Linewidth dependent on time duration T with $I = 0.8$ nW/mm². The blue circles are the measurement data for the $^3P_0\ F = 1/2 \rightarrow ^3D_1\ F = 1/2$ transition and the red circles are the measurement data for the $^3P_0\ F = 1/2 \rightarrow ^3D_1\ F = 3/2$ transition. Each point has been measured four times. The corresponding data are fitted with the function $\frac{1}{2\pi\gamma}\sqrt{1 + \frac{T}{I_s}} + c$ for (a) and $kT + c$ for (b), where $I_s = 0.24$ μ W/mm² is the saturated intensity. By fitting the spectra of the $6s6p\ ^3P_0\ (F = 1/2) \rightarrow 5d6s\ ^3D_1\ (F = 1/2, 3/2)$ transitions with the Lorentzian function, we show that the linewidths are 0.705 MHz for (c) and 0.800 MHz for (d).

the spectra is recorded as an individual data point in Fig. 4. According to the f_c under different experimental conditions, we can evaluate the frequency shifts such as the lattice light shift, the Zeeman shift, the density shift, and the 1389-nm probe light shift. Table II gives the systematic frequency shifts with their associated uncertainties for the $6s6p\ ^3P_0\ (F = 1/2) \rightarrow 5d6s\ ^3D_1\ (F = 1/2, 3/2)$ transitions.

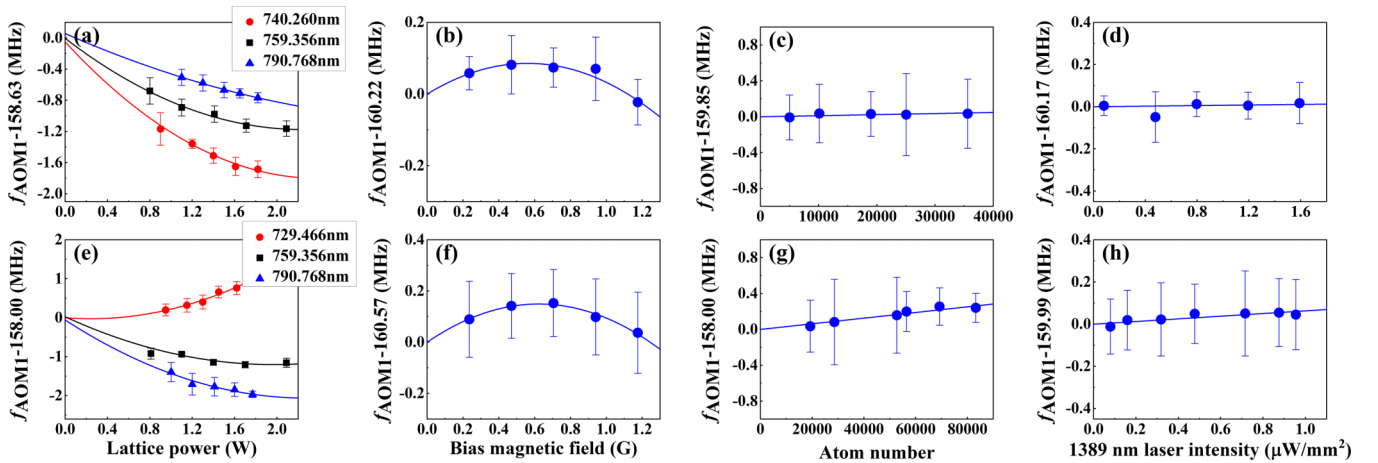


FIG. 4. Frequency shifts and uncertainties measurements. Measuring (a) relative transition shifts as a function of the lattice power at different lattice frequencies, (b) Zeeman shifts, (c) relative transition shifts as a function of the atom number, (d) probe Stark shifts as a function of the 1389-nm laser intensity for the $^3P_0\ F = 1/2 \rightarrow ^3D_1\ F = 1/2$ transition and (e)–(h) for the $^3P_0\ F = 1/2 \rightarrow ^3D_1\ F = 3/2$ transition.

Trapping atoms in an optical lattice will induce a lattice Stark shift for a given transition [31]. For a given state in the presence of an electric field, the lattice light shift is given by [32]

$$\Delta\nu = -\alpha U - \beta U^2, \quad (2)$$

where U is the trap depth for the lattice and is proportional to the lattice intensity. We measure the relative shifts for the transitions as a function of lattice power at different lattice frequencies. Following Eq. (2), the lattice light shift $\Delta\nu$ will vanish when the lattice power is zero. This means that the power dependence curves at different lattice frequencies should intersect at one point at zero lattice intensity. However, as shown in Figs. 4(a) and 4(e), we obtain three zero-intensity frequencies for each transition in our actual measurements, which may be derived from the statistical uncertainty of the measurement. We take the standard deviation of the obtained three zero-intensity frequencies as the uncertainty of the lattice light shift. Thus, the lattice light shifts can be determined as -1170 ± 54 kHz for the $6s6p\ ^3P_0\ (F = 1/2) \rightarrow 5d6s\ ^3D_1\ (F = 1/2)$ transition, and as -1197 ± 52 kHz for the $6s6p\ ^3P_0\ (F = 1/2) \rightarrow 5d6s\ ^3D_1\ (F = 3/2)$ transition with ~ 2 W of operating lattice power and a 394.798-THz lattice frequency.

With a nonzero magnetic field environment, magnetic field B will induce a shift in an atomic transition frequency. Including both first- and second-order Zeeman shifts, a magnetic field B gives a shift [33]

$$\Delta\nu_B = m_F \delta_g \mu_0 B + aB^2, \quad (3)$$

where δ_g is the difference in the g factor of the transition states. We measure the transition shifts as a function of B to determine the Zeeman shift arising from the bias magnetic field. The resulting data shown in Figs. 4(b) and 4(f) are fitted with $aB^2 + bB$. Therefore, we determine that the first-order sensitivity is 306 ± 84 kHz/kHz/G and the second-order sensitivity is -274 ± 61 kHz/G² for the $6s6p\ ^3P_0\ (F = 1/2) \rightarrow 5d6s\ ^3D_1\ (F = 1/2)$ transition, and 480 ± 72 kHz/kHz/G

TABLE II. Transition frequency shifts and uncertainties budget.

Effect	$6s6p\ ^3P_0\ F = 1/2 \rightarrow 5d6s\ ^3D_1\ F = 1/2$		$6s6p\ ^3P_0\ F = 1/2 \rightarrow 5d6s\ ^3D_1\ F = 3/2$	
	Shift(kHz)	Uncertainty(kHz)	Shift(kHz)	Uncertainty(kHz)
Lattice Stark	-1170	54	-1197	52
First-order Zeeman	72	20	113	17
Second-order Zeeman	-15	3	-21	3
Density	43	28	112	21
Probe Stark	1	1	5	1
Total	-1069	64	-988	59

and -385 ± 50 kHz/G² for the $6s6p\ ^3P_0\ (F = 1/2) \rightarrow 5d6s\ ^3D_1\ (F = 3/2)$ transition.

Large atom density in the optical lattice will yield significant atomic interactions that will perturb the atomic transition frequency [34,35]. The shift is proportional to the atomic density [36], thus we investigate the density-induced frequency shift by varying the atom number loaded into the optical lattice. The atom number is reduced by a variation of the laser power for the Zeeman slower. The density shift as a function of different atom numbers is shown in Figs. 4(c) and 4(g). Extrapolating this measurement result to the zero atomic number, we obtain the sensitivity of the density shift: 1.2 ± 0.8 Hz/atom and 3.2 ± 0.6 Hz/atom for the $6s6p\ ^3P_0\ (F = 1/2) \rightarrow 5d6s\ ^3D_1\ (F = 1/2)$ and the $6s6p\ ^3P_0\ (F = 1/2) \rightarrow 5d6s\ ^3D_1\ (F = 3/2)$ transitions.

The probe ac Stark shift, which is caused by the 1389-nm laser, is proportional to the probe laser intensity I [37],

$$\Delta\nu = KI, \quad (4)$$

as shown in Figs. 4(d) and 4(h), the effect of the 1389-nm laser power on the $6s6p\ ^3P_0\ (F = 1/2) \rightarrow 5d6s\ ^3D_1\ (F = 1/2, 3/2)$ transition frequencies is explored within the intensity range around $(0.3 \text{ to } 6.7) I_s$, while keeping the duration of 1389-nm laser pulse constant. It is determined that $K = 7 \pm 15$ kHz/($\mu\text{W}/\text{mm}^2$) and $K = 63 \pm 17$ kHz/($\mu\text{W}/\text{mm}^2$) for the $6s6p\ ^3P_0\ (F = 1/2) \rightarrow 5d6s\ ^3D_1\ (F = 1/2)$ and the $6s6p\ ^3P_0\ (F = 1/2) \rightarrow 5d6s\ ^3D_1\ (F = 3/2)$ transitions, respectively.

IV. ABSOLUTE FREQUENCIES AND HYPERFINE CONSTANT

A commercial optical frequency comb from the Menlo systems is employed to measure the frequency of the laser. As shown in Fig. 2(a), the frequency of the 1389-nm laser is referenced to an absolute frequency-stabilized optical frequency comb. The comb's repetition frequency f_{rep} is referenced on a 578-nm ultrastable clock laser. The offset frequency f_{CEO} of the comb is locked to an H-maser. The frequency of the 578-nm laser at the frequency comb f_{578} is

$$f_{578} = \pm 2f_{\text{CEO}} + n_1 f_{\text{rep}} \pm f_{578\text{beat}}. \quad (5)$$

Similarly, the frequency of the 1389-nm laser at the frequency comb f_{1389} is

$$f_{1389} = \pm f_{\text{CEO}} + n_2 f_{\text{rep}} \pm f_{1389\text{beat}}, \quad (6)$$

where $f_{578\text{beat}}$ or $f_{1389\text{beat}}$ is the heterodyne beat between the 578-nm or 1389-nm laser and the comb, and n_i is the integer

of the comb mode number. The f_{rep} , $f_{578\text{beat}}$, and $f_{1389\text{beat}}$ are measured by the frequency counter respectively. Consequently, we could determine the f_{578} and f_{1389} according to Eqs. (5) and (6).

To determine the absolute frequencies for a given transition, it is necessary to trace the frequency measurement results to the International System of Units (SI) second. Since the clock transition of ^{171}Yb is the secondary representation of the SI second, its absolute frequency is well known. We could determine the absolute frequency of the $6s6p\ ^3P_0\ (F = 1/2) \rightarrow 5d6s\ ^3D_1\ (F = 1/2, 3/2)$ transitions against an H-maser through the comb, which is corrected by the absolute frequency of the ^{171}Yb clock transition. For each measurement, we probe the clock transition spectra of ^{171}Yb with a linewidth at a few Hz. Then we compare the frequency of the clock transition measured by the comb with the 2017 the International Committee for Weights and Measures-recommended absolute frequency of 518 295 836 590 863.6 Hz [6], and a frequency difference of about $\Delta\nu_{578} = -1.71$ kHz is obtained.

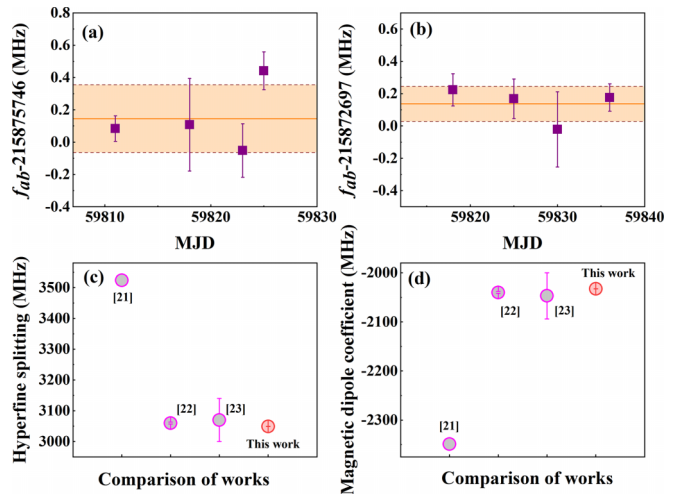


FIG. 5. The absolute frequencies measurement of the $6s6p\ ^3P_0\ (F = 1/2) \rightarrow 5d6s\ ^3D_1\ (F = 1/2, 3/2)$ transitions for (a) the $^3P_0\ F = 1/2 \rightarrow ^3D_1\ F = 1/2$ transition and (b) the $^3P_0\ F = 1/2 \rightarrow ^3D_1\ F = 3/2$ transition. Both transitions are measured four times. The absolute frequencies are determined by averaging the results of the four measurements and are indicated by the orange solid lines. The light orange shading represents the corresponding statistical uncertainties. The present measurement results for the hyperfine splitting (c) and the magnetic dipole A coefficient (d) of the 3D_1 state are compared with previous theory and experiment results.

Therefore, the correction for the 1389-nm optical frequency is $\Delta\nu_c = -0.71$ kHz. The absolute frequencies f_{ab} of the $6s6p\ ^3P_0$ ($F = 1/2$) \rightarrow $5d6s\ ^3D_1$ ($F = 1/2, 3/2$) transitions are determined by

$$f_{ab} = f_{1389} - f_c + \Delta\nu_{\text{sys}} + \Delta\nu_c, \quad (7)$$

where $\Delta\nu_{\text{sys}}$ is the systematic frequency shifts for individual measurement. We perform four measurements for both transitions and take the average value as the final absolute frequency results, as shown in Figs. 5(a) and 5(b), the corresponding standard deviation is taken as the statistical uncertainty. The error bar for each data point is contributed by a combination of statistical and systematic uncertainties. The statistical uncertainty mainly comes from multiple measurements for the center frequency of the transition spectra. According to the absolute frequency measurement results of the two hyperfine transitions, the corresponding hyperfine splitting and the magnetic dipole A coefficient for the $5d6s\ ^3D_1$ state can be acquired as 3049.01(26) MHz and 2032.67(17) MHz. Figures 5(c) and 5(d) plots our results.

V. CONCLUSION

In conclusion, by referencing the secondary representation of the SI second and evaluating the systematic frequency shifts in detail, we have directly measured the absolute frequency of the 1389-nm repumping transition of the ^{171}Yb atomic optical clock. The absolute frequencies are $215\,875\,746.15 \pm (0.21)_{\text{stat}} \pm (0.06)_{\text{sys}}$ MHz for the $6s6p\ ^3P_0$ $F = 1/2 \rightarrow 5d6s\ ^3D_1$ $F = 1/2$ transition and $215\,872\,697.14 \pm$

$(0.11)_{\text{stat}} \pm (0.06)_{\text{sys}}$ MHz for the $6s6p\ ^3P_0$ $F = 1/2 \rightarrow 5d6s\ ^3D_1$ $F = 3/2$ transition. The uncertainty is mainly derived from the statistical uncertainty arising from multiple measurements of the transition frequency. According to the absolute frequencies measurement results, the hyperfine splitting and the magnetic dipole coefficient A is determined, which is one order of magnitude more accurate than the previous measurements. Therefore, it can provide a much more accurate reference for theoretical calculations. Moreover, as the $6s6p\ ^3P_0 \rightarrow 5d6s\ ^3D_1$ transition is the repumping channel for the ^{171}Yb optical clock, adequate knowledge of the absolute frequency of the transition, not only can help us promote the efficiency of repumping the atoms, but also could reduce the laser power demand on the repumper during the clock interrogation. This will contribute to reducing the power consumption of the optical clock system for further applications in environments such as transportable or space stations.

ACKNOWLEDGMENTS

This work is supported by the National Natural Science Foundation of China (Grants No. 62105102 and No. 11134003), the National Key Research and Development Program of China (Grants No. 2016YFA0302103, No. 2017YFF0212003, and No. 2016YFB0501601), the Shanghai Municipal Science and Technology Major Project (Grant No. 2019SHZDZX01, and the Shanghai Excellent Academic Leaders Program (Grant No. 12XD1402400).

-
- [1] X. Zheng, J. Dolde, V. Lochab, B. N. Merriman, H. R. Li, and S. Kolkowitz, *Nature (London)* **602**, 425 (2022).
 - [2] T. Bothwell, C. J. Kennedy, A. Aeppli, D. Kedar, J. M. Robinson, E. Oelker, A. Staron, and J. Ye, *Nature (London)* **602**, 420 (2022).
 - [3] T. L. Nicholson, S. L. Campbell, R. B. Hutson, G. E. Marti, B. J. Bloom, R. L. McNally, W. Zhang, M. D. Barrett, M. S. Safronova, G. F. Strouse, W. L. Tew, and J. Ye, *Nat. Commun.* **6**, 6896 (2015).
 - [4] T. Bothwell, D. Kedar, E. Oelker, J. M. Robinson, S. L. Bromley, W. L. Tew, J. Ye, and C. J. Kennedy, *Metrologia* **56**, 065004 (2019).
 - [5] W. F. McGrew, X. Zhang, R. J. Fasano, S. A. Schäffer, K. Beloy, D. Nicolodi, R. C. Brown, N. Hinkley, G. Milani, M. Schioppo, T. H. Yoon, and A. D. Ludlow, *Nature (London)* **564**, 87 (2018).
 - [6] F. Riehle, P. Gill, F. Arias, and L. Robertsson, *Metrologia* **55**, 188 (2018).
 - [7] X. B. Zhang and J. Ye, *Natl. Sci. Rev.* **3**, 189 (2016).
 - [8] R. Le Targat, L. Lorini, Y. Le Coq, M. Zawada, J. Guéna, M. Abgrall, M. Gurov, P. Rosenbusch, D. G. Rovera, B. Nagórny, R. Gartman, P. G. Westergaard, M. E. Tobar, M. Lours, G. Santarelli, A. Clairon, S. Bize, P. Laurent, P. Lemonde, and J. Lodewyck, *Nat. Commun.* **4**, 2109 (2013).
 - [9] Boulder Atomic Clock Optical Network (BACON) Collaboration, *Nature (London)* **591**, 564 (2021).
 - [10] T. E. Mehlstäubler, G. Grosche, C. Lisdat, P. O. Schmidt, and H. Denker, *Rep. Prog. Phys.* **81**, 064401 (2018).
 - [11] C. W. Chou, D. B. Hume, T. Rosenband, and D. J. Wineland, *Science* **329**, 1630 (2010).
 - [12] M. Takamoto, I. Ushijima, N. Ohmae, T. Yahagi, K. Kokado, H. Shinkai, and H. Katori, *Nat. Photonics* **14**, 411 (2020).
 - [13] T. Rosenband, D. B. Hume, P. O. Schmidt, C. W. Chou, A. Brusch, L. Lorini, W. H. Oskay, R. E. Drullinger, T. M. Fortier, J. E. Stalnaker, S. A. Diddams, W. C. Swann, N. R. Newbury, W. M. Itano, D. J. Wineland, and J. C. Bergquist, *Science* **319**, 1808 (2008).
 - [14] R. Lange, N. Huntemann, J. M. Rahm, C. Sanner, H. Shao, B. Lipphardt, Chr. Tamm, S. Weyers, and E. Peik, *Phys. Rev. Lett.* **126**, 011102 (2021).
 - [15] A. Derevianko and M. Pospelov, *Nat. Phys.* **10**, 933 (2014).
 - [16] M. S. Safronova, D. Budker, D. DeMille, D. F. J. Kimball, A. Derevianko, and C. W. Clark, *Rev. Mod. Phys.* **90**, 025008 (2018).
 - [17] A. D. Ludlow, M. M. Boyd, J. Ye, E. Peik, and P. O. Schmidt, *Rev. Mod. Phys.* **87**, 637 (2015).
 - [18] N. Nemitz, T. Ohkubo, M. Takamoto, I. Ushijima, M. Das, N. Ohmae, and H. Katori, *Nat. Photon.* **10**, 258 (2016).
 - [19] N. Hinkley, J. A. Sherman, N. B. Phillips, M. Schioppo, N. D. Lemke, K. Beloy, M. Pizzocaro, C. W. Oates, and A. D. Ludlow, *Science* **341**, 1215 (2013).

- [20] E. Arimondo, M. Inguscio, and P. Violino, *Rev. Mod. Phys.* **49**, 31 (1977).
- [21] M. G. Kozlov, V. A. Dzuba, and V. V. Flambaum, *Phys. Rev. A* **99**, 012516 (2019).
- [22] C. J. Bowers, D. Budker, S. J. Freedman, G. Gwinner, J. E. Stalnaker, and D. DeMille, *Phys. Rev. A* **59**, 3513 (1999).
- [23] K. Beloy, J. A. Sherman, N. D. Lemke, N. Hinkley, C. W. Oates, and A. D. Ludlow, *Phys. Rev. A* **86**, 051404(R) (2012).
- [24] L. M. Luo, H. Qiao, D. Ai, M. Zhou, S. Zhang, S. Zhang, C. Y. Sun, Q. C. Qi, C. Q. Peng, T. Y. Jin, W. Fang, Z. Q. Yang, T. C. Li, K. Liang, and X. Y. Xu, *Metrologia* **57**, 065017 (2020).
- [25] Q. Gao, M. Zhou, C. Y. Han, S. Y. Li, S. Zhang, Y. Yao, B. Li, H. Qiao, D. Ai, G. Lou, M. Y. Zhang, Y. Y. Jiang, Z. Y. Bi, L. S. Ma, and X. Y. Xu, *Sci. Rep.* **8**, 8022 (2018).
- [26] W. Nagourney, J. Sandberg, and H. Dehmelt, *Phys. Rev. Lett.* **56**, 2797 (1986).
- [27] S. Zhang, H. Qiao, D. Ai, M. Zhou, and X. Y. Xu, *Laser Phys. Lett.* **19**, 095701 (2022).
- [28] D. Ai, H. Qiao, S. Zhang, L. M. Luo, C. Y. Sun, S. Zhang, C. Q. Peng, Q. C. Qi, T. Y. Jin, M. Zhou, and X. Y. Xu, *Chin. Phys. B* **29**, 090601 (2020).
- [29] W. F. McGrew, X. Zhang, H. Leopardi, R. J. Fasano, D. Nicolodi, K. Beloy, J. Yao, J. A. Sherman, S. A. Schäffer, J. Savory, R. C. Brown, S. Römisch, C. W. Oates, T. E. Parker, T. M. Fortier, and A. D. Ludlow, *Optica* **6**, 448 (2019).
- [30] N. Ohmae, F. Bregolin, N. Nemitz, and H. Katori, *Opt. Express* **28**, 15112 (2020).
- [31] H. Katori, M. Takamoto, V. G. Pal'chikov, and V. D. Ovsiannikov, *Phys. Rev. Lett.* **91**, 173005 (2003).
- [32] R. C. Brown, N. B. Phillips, K. Beloy, W. F. McGrew, M. Schioppo, R. J. Fasano, G. Milani, X. Zhang, N. Hinkley, H. Leopardi, T. H. Yoon, D. Nicolodi, T. M. Fortier, and A. D. Ludlow, *Phys. Rev. Lett.* **119**, 253001 (2017).
- [33] M. M. Boyd, T. Zelevinsky, A. D. Ludlow, S. Blatt, T. Zanon-Willette, S. M. Foreman, and J. Ye, *Phys. Rev. A* **76**, 022510 (2007).
- [34] M. J. Martin, M. Bishof, M. D. Swallows, X. Zhang, C. Benko, J. von-Stecher, A. V. Gorshkov, A. M. Rey, and Jun Ye, *Science* **341**, 632 (2013).
- [35] G. K. Campbell, M. M. Boyd, J. W. Thomsen, M. J. Martin, S. Blatt, M. D. Swallows, T. L. Nicholson, T. Fortier, C. W. Oates, S. A. Diddams, N. D. Lemke, P. Naidon, P. Julienne, J. Ye, and A. D. Ludlow, *Science* **324**, 360 (2009).
- [36] M. W. Zwiernik, Z. Hadzibabic, S. Gupta, and W. Ketterle, *Phys. Rev. Lett.* **91**, 250404 (2003).
- [37] N. Poli, Z. W. Barber, N. D. Lemke, C. W. Oates, L. S. Ma, J. E. Stalnaker, T. M. Fortier, S. A. Diddams, L. Hollberg, J. C. Bergquist, A. Brusch, S. Jefferts, T. Heavner, and T. Parker, *Phys. Rev. A* **77**, 050501(R) (2008).